

## Surface-enhanced Raman spectroscopy employing monodisperse nickel nanowire arrays

G. Sauer, G. Brehm, and S. Schneider

*Institute of Physical and Theoretical Chemistry, University of Erlangen, Egerlandstrasse 3, D-91058 Erlangen, Germany*

H. Graener and G. Seifert

*Department of Physics, Martin-Luther University of Halle-Wittenberg, 06108 Halle, Germany*

K. Nielsch, J. Choi, P. Göring, and U. Gösele

*Max-Planck-Institute of Microstructure Physics, 06120 Halle, Germany*

P. Miclea and R. B. Wehrspohn<sup>a)</sup>

*Department of Physics, University of Paderborn, 33095 Paderborn, Germany*

(Received 16 August 2005; accepted 9 November 2005; published online 10 January 2006)

We have prepared two-dimensional arrays of hexagonally arranged, monodisperse nickel nanowires embedded in an alumina template. The degree of template filling is nearly 100% using an improved electrochemical deposition technique. Optical transmission measurements in the direction parallel to the long axis of the nickel nanowires show a plasmon-enhanced absorption around 400 nm. We observe for typically surface-enhanced Raman spectroscopy (SERS) inactive metals like nickel a strong, but locally strongly inhomogeneous SERS signal during *in situ* Raman microspectroscopy. Supported by our numerical modeling, we suggest that significant SERS enhancement factors are possible only when nanowires in bundles are touching each other. © 2006 American Institute of Physics. [DOI: 10.1063/1.2162682]

The emerging area of plasmonics has considered noble metals mainly as a working horse. However, there is no reason to restrict the material system to gold, silver, and copper since there are a lot more metals that have, in addition to the plasmon resonance, other interesting optical properties. For example, ferromagnetic metals such as nickel or cobalt are known to have a spectral position of the plasmon resonance similar to that of silver and, in addition, they exhibit interesting magneto-optical properties. The combination of magnetic properties such as the ferromagnetic resonance with plasmonic resonances may lead in the future to a new class of tuneable metamaterials.<sup>1</sup> For example, we were able to show that nickel nanowire arrays exhibit a ferromagnetic resonance at around 9.4 MHz, corresponding to a region of negative permeability.<sup>2</sup> We were also able to show that magneto-optical Kerr effect in nickel nanowire arrays is enhanced by localized plasmons.<sup>3</sup> It has also been shown by us recently that silver nanowire arrays can be used as a model system for surface-enhanced Raman scattering (SERS) since the enhancement factor scales linearly with the surface of the wire<sup>4</sup> being in contact to the analyte. Here, we will show that SERS can also be observed on nickel nanowire arrays. The observed enhancement factors do agree well with analytic models based on the work by Genov *et al.* in 2004.<sup>5</sup> We believe that these findings open a new route for optical metamaterials in the area of sensing.

Surface-enhanced Raman scattering is generally applied to the detection or sensing of ultralow concentrations of molecules.<sup>6</sup> When molecules are adsorbed at coinage metal nanoparticles, the Raman signal of the adsorbed species can be enhanced by several orders of magnitude due to the interaction with the nanoparticle. This enormous enhancement is

commonly explained by a combination of two mechanisms: a minor contribution from the charge transfer mechanism and the major contribution from the electromagnetic (EM) mechanism. Therefore, SERS measurements on well-defined nanoparticle systems are well suited to probe the local electromagnetic field on the surface of the nanoparticle. According to EM theory, the enhancement of a given electromagnetic field in close vicinity of a nanoparticle critically depends on the nanoparticle size, shape, and orientation with respect to the incoming field.<sup>7</sup> Many SERS systems are currently either based on roughened metal surfaces or colloidal metal particles. In both cases, the electromagnetic field enhancement cannot be easily determined. We have recently described the use of metal nanowire arrays as a model system for SERS spectroscopy and concluded that the enhancement factor is clearly dominated by the electromagnetic mechanism.<sup>4</sup> To date, only one group reported SERS on transition metal nanowires.<sup>8,9</sup> However, the templates used were disordered and had a wide pore size distribution. From the experimental details given, one can conclude that the homogeneity of the metal filling was quite poor. Therefore, the intensities of space-averaged SERS signals are likely to vary locally making the interpretation of the SERS data difficult. In contrast to the studies just mentioned, in our experiments we use highly ordered arrays of monodisperse nanowires with adjustable but well-defined diameter and length.

The preparation of highly ordered nickel nanowire arrays is described in detail in Refs. 10 and 11. In all experiments described, the nanowires had a diameter of about 40 nm and an initial length of approximately 2  $\mu\text{m}$ , corresponding to an aspect ratio of 50. Prior to the optical measurements, nickel deposited in excess on the top of template and the dendritic structure on the bottom was removed by ion milling. By employing this procedure, it was ensured that

<sup>a)</sup>Electronic mail: wehrspohn@physik.upb.de

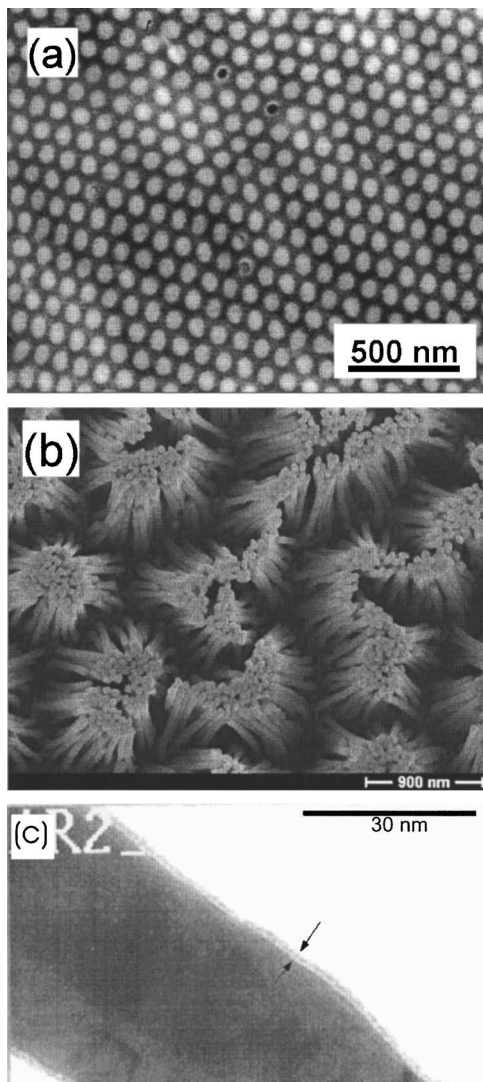


FIG. 1. (a) Scanning electron micrograph of a nickel nanowire array embedded in the porous alumina template. (b) Same sample after selectively dissolving the template (parameters). (c) Transmission electron micrograph of a nickel nanowire after selectively dissolving the template. The nickel oxide layer has a thickness of about 2 nm.

highly uniform samples are obtained [Fig. 1(a)].

The optical properties of ordered arrays of porous alumina have been studied by us in detail in Ref. 12. For the optical measurements, the as-filled template has been glued on a copper ring (inner diameter=1.5 mm) and the aluminum on the backside of the template has been selectively dissolved in a  $\text{CuCl}_2/\text{HCl}$  solution. Both sides of the filled template have been thinned by ion milling to remove the dendritic metal filling on the one side and possible metal deposition on the top of the template on the other side. The ion-milling time determines the final thickness of the filled template. Figure 2 shows a typical extinction spectrum of a highly ordered ensemble of nickel nanowires. The parameters are pore diameter  $D_p \approx 40$  nm and interpore distance  $D_{\text{int}} \approx 110$  nm. The propagation direction of the white light is perpendicular to the surface, that is, parallel to the long axis of the nanowire. The electric field is therefore perpendicular to the long axis of the nanowire. We performed calculations based on Mie's theory.<sup>13</sup> Since the electric field is in this configuration strictly perpendicular to the long axis of the wire, the generalized Lorenz-Mie theory can be applied. The

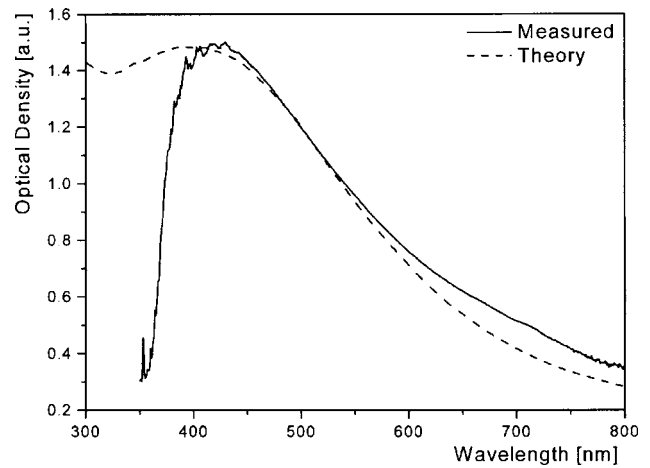


FIG. 2. Experimentally determined extinction spectra for ordered nickel nanowire ensembles with a diameter  $D_p \approx 40$  nm and interwire distance  $D_{\text{int}} \approx 110$  nm embedded in an alumina matrix (solid line). Calculated extinction spectra for nickel nanoparticles with a diameter  $D_p \approx 40$  nm embedded in an alumina matrix with  $\epsilon_m = 2.5$  (dashed line).

dielectric function of nickel bulk materials was taken from.<sup>14</sup> Figure 2 shows a numerical simulation of the extinction spectrum for spherical particles with  $D_p = 40$  nm embedded in an porous alumina matrix ( $\epsilon_m = 2.5$ ). The peak position of the plasmon resonance at around 400 nm as well as the shape and relative magnitude of the nickel samples correspond reasonably well to the experimental results. The cutoff of the experimental spectrum at around 400 nm is due to the limited spectral range of the optical setup.

SERS spectra were taken with a home-built Raman microscope [excitation wavelength  $\lambda_{\text{exc}} = 632.8$  nm, laser power  $\leq 5$  mW at the sample, microscope lens:  $50\times$ , numerical aperture of 0.5 (allowing a spatial resolution of a few  $\mu\text{m}$ )]. We used pyridine as standard analyte since it does not exhibit any resonance enhancements. If a  $10^{-2}$  M solution of pyridine in 0.1 M KCl is brought into contact with a nickel nanowire array embedded in an alumina template no signal of the probe molecules can be detected. This finding is not very surprising as it agrees very well with the findings for silver,<sup>4</sup> especially when considering the expected low enhancement factor of nickel surfaces. However, if the  $10^{-2}$  M solution is brought into contact with a Ni nanowire array after partially creating freestanding nanowires by etching with  $\text{H}_3\text{PO}_4$  [see Fig. 1(b)], the situation changes dramatically. Although on most locations no Raman bands can be detected (Fig. 3, bottom spectrum), on distinct locations intense pyridine SERS spectra appear. Although the absolute value of the SERS enhancement factor is difficult to quantify, it is obvious that it varies locally by two to three orders of magnitude.

To analyze this surprising enhancement factor, we calculated first the enhancement factor of a single nanowire based on the theory developed by Kerker *et al.*<sup>15</sup> When the excitation light is propagating parallel to the wire axis and the molecules are aligned perpendicular to the wire axis, the small-particle limit for spherical particles can be used. The enhancement factor is given by<sup>16</sup>

$$G = \left| 1 + 2 \frac{D_p^3}{r'^3} g_0 + 2 \frac{D_p^6}{r'^6} g_0 g_0 + 3 \frac{D_p^3}{r'^3} g \right|^2, \quad (1)$$

where  $g$  and  $g_0$  are the values of the function  $(\epsilon_m - \epsilon_d)/(\epsilon_m + 2\epsilon_d)$  at the Raman-shifted frequency and the ex-

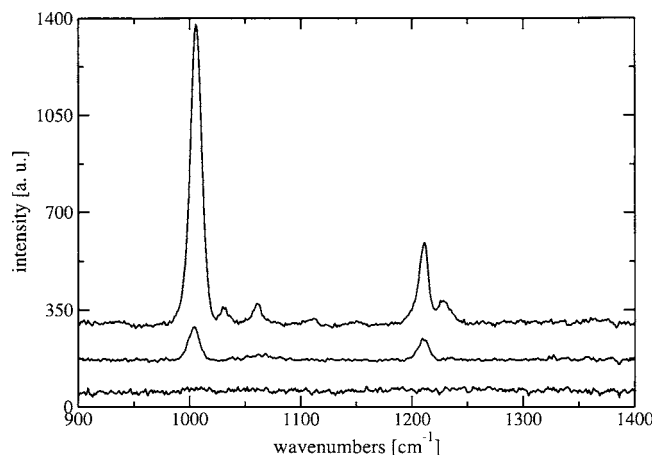


FIG. 3. SERS spectra of pyridine @Ni nanowires recorded with  $\lambda_{\text{exc}} = 632.8$  nm at different locations on the sample in Fig. 1(b) (shifted for clarity).

citation frequency, respectively.  $D_p$  is the radius of the wire and  $r'$  is the distance of the molecule from the center of the wire. If the molecule is directly on the metal surface,  $D_p = r'$ . If there is, however, an oxide layer between the metal and the molecule,  $r' = D_p + h$ , where  $h$  is the separation distance. Equation (1) leads to theoretical enhancement factors of  $G=50$  to  $100$  for nickel nanowires of a width of  $40$  nm at  $\lambda = 632.8$  nm depending on the separation distance  $h$ . Assuming a typical nickel oxide thickness of  $2$  nm as determined from Fig. 1(c), we expect no significant SERS enhancement from single nickel nanowires.

In order to analyze the effect of coupled nanowires, we used the recently developed analytic model for periodically arranged nanowire arrays by Genov *et al.*<sup>5</sup> In this model, the ensemble effect is calculated, not the single nanowire SERS enhancement. The SERS enhancement factor is plotted as a function of the parameter  $\gamma$ , which is a relative measure of the interwire distance  $\gamma = D_p / (D_{\text{int}} - D_p)$  (Fig. 4). The analytical relation from Genov *et al.*<sup>5</sup> for  $\gamma \gg 1$  reads

$$G \approx \frac{\pi(m+1)^{7/2}}{2((4-\pi)m+4)\kappa^{7/2}} \times \sqrt{\frac{4\Delta^2+9}{(\Delta^2+1)^{3/2}} - \frac{\Delta(4\Delta^4+15\Delta^2+15)}{(\Delta^2+1)^3}}, \quad (2)$$

where  $m = |\epsilon'_m| / \epsilon_d$ , with  $\epsilon'_m$  the real part of the dielectric function of the metal,  $\epsilon_d$  the dielectric function of the dielectric matrix,  $\kappa$  the loss factor, and  $\Delta = (m/\gamma - 1)/\kappa$ .

As it becomes obvious from Fig. 1(b), in the case where the wires have substantially been released from the alumina matrix, they form bundles and the interwire spacing can become locally very small. For example, if we assume that two Ni nanowires with a  $2$  nm oxide layer are touching,  $\gamma = 10$ . According to Fig. 4 this leads to a SERS enhancement factor of  $G \approx 400$  in line with our experimental measurements. Similar field-enhancement configurations are also possible on roughened nickel electrodes and might explain the observed Raman enhancement.<sup>17</sup>

In summary, we prepared in a very well-controlled manner two-dimensional arrays of hexagonally arranged, mono-

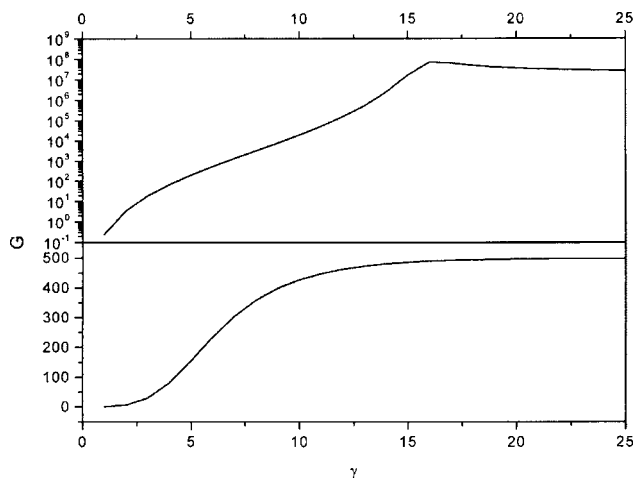


FIG. 4. Estimated electromagnetic enhancement factor for Ag (top) and Ni (bottom) nanowires as a function of the interwire distance  $\gamma$  for  $40$  nm diameter and  $632.8$  nm wavelength. The matrix is assumed to be an aqueous solution ( $\epsilon_m = 1.76$ ).

disperse nickel nanowires embedded in an alumina matrix. The dimensions of the nanowires can be adjusted by the template (wire diameter and length). The extinction spectra of these nanowire arrays were determined and compared with theory. We confirmed the first observation of SERS on Ni nanowire arrays by Yao *et al.*<sup>8</sup> *In situ* measurements showed that a significant SERS enhancement is only observed at certain hot spots of partially released nanowire bundles. The enhancement might be related to Ni nanowires touching each other in the bundles. This hypothesis is supported by analytically modeling of the SERS enhancement factor. Typical enhancement factors of about two to three orders of magnitude were observed and calculated.

<sup>1</sup>S. Chui, Z. Lin, and L. Hu, Phys. Lett. A **319**, 85 (2003).

<sup>2</sup>C. Ramos, M. Vasquez, K. Nielsch, K. Pirota, J. Rivas, R. Wehrspohn, M. Tovar, R. Sanchez, and U. Gösele, J. Magn. Magn. Mater. **272–276**, 1652 (2004).

<sup>3</sup>S. Melle, J. Menendez, G. Armelles, D. Navas, M. Vasquez, K. Nielsch, R. Wehrspohn, and U. Gösele, Appl. Phys. Lett. **83**, 4547 (2003).

<sup>4</sup>G. Sauer, G. Brehm, S. Schneider, H. Graener, G. Seifert, K. Nielsch, J. Choi, P. Göring, U. Gösele, P. Miclea, and R. B. Wehrspohn, J. Appl. Phys. **97**, 024308 (2005).

<sup>5</sup>D. Genov, A. Arychev, V. Shalaev, and A. Wei, Nano Lett. **4**, 153 (2004).

<sup>6</sup>K. Kneipp, H. Kneipp, I. Itzkan, R. R. Dasari, and M. S. Feld, J. Phys.: Condens. Matter **14**, R597 (2002).

<sup>7</sup>C. L. Haynes and R. P. Van Duyne, J. Phys. Chem. B **105**, 5599 (2001).

<sup>8</sup>J. L. Yao, J. Tang, D. Y. Wu, D. M. Sun, K. H. Xue, B. Ren, B. W. Mao, and Z. Q. Tian, Surf. Sci. **514**, 108 (2002).

<sup>9</sup>Z. Q. Tian, B. Ren, and D. Y. Wu, J. Phys. Chem. B **106**, 9463 (2002).

<sup>10</sup>K. Nielsch, R. Wehrspohn, J. Barthel, J. Kirschner, U. Gösele, S. F. Fischer, and H. Kronmüller, Appl. Phys. Lett. **79**, 1360 (2001).

<sup>11</sup>G. Sauer, G. Brehm, S. Schneider, K. Nielsch, R. B. Wehrspohn, J. Choi, H. Hofmeister, and U. Gösele, J. Appl. Phys. **91**, 3243 (2002).

<sup>12</sup>J. Choi, Y. Luo, R. B. Wehrspohn, R. Hillebrand, J. Schilling, and U. Gösele, Appl. Phys. Lett. **83**, 3036 (2003).

<sup>13</sup>U. Kreibig and M. Vollmer, *Optical Properties of Metal Clusters* (Springer, Berlin, 1995).

<sup>14</sup>*Handbook of Optical Constants of Solids*, edited by E. D. Palik (Academic, Boston, 1985).

<sup>15</sup>M. Kerker, D. Wang, and H. Chew, Appl. Opt. **19**, 4159 (1980).

<sup>16</sup>M. Moskovits, Rev. Mod. Phys. **57**, 783 (1985).

<sup>17</sup>Q. Huang, X. Lin, Z. Yang, J. Hu, and Z. Q. Tian, J. Electroanal. Chem. **563**, 121 (2004).